Codelivery of VEGF siRNA and Gemcitabine Monophosphate in a Single Nanoparticle Formulation for Effective Treatment of NSCLC

Yuan Zhang[1], Nicole MJ Schwerbrock[2], Arlin B Rogers[3], William Y Kim[4] and Leaf Huang[1]

[1]Division of Molecular Pharmaceutics and Center for Nanotechnology in Drug Delivery, Eshelman School of Pharmacy, University of North Carolina at Chapel Hill, Chapel Hill, North Carolina, USA; [2]Qualiber Inc., Chapel Hill, North Carolina, USA; [3]Department of Pathology and Laboratory Medicine, School of Medicine, University of North Carolina at Chapel Hill, Chapel Hill, North Carolina, USA; [4]Lineberger Comprehensive Cancer Center, University of North Carolina at Chapel Hill, Chapel Hill, North Carolina, USA

There is an urgent need for new therapeutics for the treatment of aggressive and metastatic refractory human non-small–cell lung cancer (NSCLC). Antiangiogenesis therapy and chemotherapy are the two major treatment options. Unfortunately, both types of therapies when used individually have their disadvantages. Integrating antiangiogenesis therapy with chemotherapy is expected to target the tumor's vascular endothelial cells and the tumor cells simultaneously. In this study, we coformulated Vascular endothelial growth factor (VEGF) siRNA targeting VEGFs and gemcitabine monophosphate (GMP) into a single cell-specific, targeted lipid/calcium/phosphate (LCP) nanoparticle formulation. Antitumor effect of the combination therapy using LCP loaded with both VEGF siRNA and GMP was evaluated in both subcutaneous and orthotopic xenograft models of NSCLC with systemic administration. The improved therapeutic response, as compared with either VEGF siRNA or GMP therapy alone, was supported by the observation of 30–40% induction of tumor cell apoptosis, eightfold reduction of tumor cell proliferation and significant decrease of tumor microvessel density (MVD). The combination therapy led to dramatic inhibition of tumor growth, with little *in vivo* toxicity. In addition, the current studies demonstrated the possibility of incorporating multiple nucleic acid molecules and phosphorylated small-molecule drugs, targeting to different pathways, into a single nanoparticle formulation for profound therapeutic effect.

Received 11 March 2013; accepted 3 May 2013; advance online publication 18 June 2013. doi:10.1038/mt.2013.120

INTRODUCTION

The combination of chemotherapy and gene therapy could greatly increase their therapeutic efficacy in the treatment of many human diseases. The drawbacks associated with standard chemotherapy regimens can be alleviated by the addition of gene therapy to the treatment plan.[1] Furthermore, the efficacy of gene therapy can be bolstered by chemo-agents whose effects are often more potent and widespread. This increase in efficacy could be particularly important in the treatment of aggressive human cancers whose progression and invasion involves a variety of physiological or pathological factors, such as non-small–cell lung cancer (NSCLC).

Antiangiogenesis therapy and chemotherapy are important treatment regimens for NSCLC. Vascular endothelial growth factor (VEGF) is overexpressed in malignant tumors and is a major driver of tumor angiogenesis. Blocking the VEGF signaling pathway can reduce tumor-associated angiogenesis and blood vessel–dependent metastasis.[2,3] VEGF-receptor (VEGFR) inhibitors, such as small-molecule inhibitors, anti-VEGF monoclonal antibodies, and aptamers that strongly antagonize the VEGF-VEGFR binding with high specificity, have been developed.[4–6] However, the efficacy of these inhibitors is often limited by unfavorable pharmacokinetics, low tumor accumulation, and undesired interaction with the immune system. Additional adverse effects also compromise the therapeutic response in patients[7,8] siRNA specific to VEGF, if properly delivered to the tumor cells, may overcome some shortcomings of the traditional drugs, especially when it is codelivered with an efficient chemodrug. Gemcitabine (2′,2′-difluoro 2′-deoxycytidine) (Gem) is a nucleoside analogue widely used as the first-line chemotherapy of advanced NSCLC. Gem relies on nucleoside transporters to enter into cells, sequentially phosphorylated by deoxycytidine kinase that forms mono-, di-, and triphosphate derivatives. The addition of the first phosphate group to become gemcitabine monophosphate (GMP) is the rate-limiting step.[9] 5′-Triphosphate derivative of Gem is then incorporated into the DNA strand where it inhibits replication by terminating the DNA chain elongation.[9]

To combine the therapeutic advantages of VEGF siRNA and Gem, while also avoiding their delivery roadblocks, we entrapped both VEGF siRNA and GMP into a single lipid/calcium/phosphate (LCP) nanoparticle formulation. Our aim was to apply multiple tumor-killing steps to programmatically inhibit tumor growth and eventually eradicate tumor progression. The small molecule ligand, anisamide (AA), was modified to the LCP surface to specifically target the sigma receptors that are overexpressed in many human cancer cells. The rational design of LCP nanoplatform lies

Correspondence: Leaf Huang, 1315 Kerr Hall CB# 7571, Chapel Hill, NC 27599-7571, USA. E-mail: leafh@email.unc.edu

in the fact that calcium ions can precipitate both siRNA and GMP. Thus, an antiangiogenic and a chemo-agents can be simultaneously delivered to the tumor cells to block different mechanisms of tumor cell proliferation (**Figure 1a**).[10] LCPs entrapping only VEGF siRNA (VEGF-LCP-AA) and LCPs entrapping only GMP (GMP-LCP-AA) were prepared and tested separately to compare with the combination therapy. Cytidine monophosphate (CMP), having a chemical structure similar to GMP, but without any cytotoxic effect, serves as the surrogate for GMP. LCPs entrapping both CMP and control siRNA ((CMP+Con)-LCP-AA) were used as control nanoparticles.

RESULTS

Characterization of drug-loaded LCPs

LCP is a membrane/core type nanoparticle. It is composed of a solid calcium phosphate precipitate core coated with a single lipid

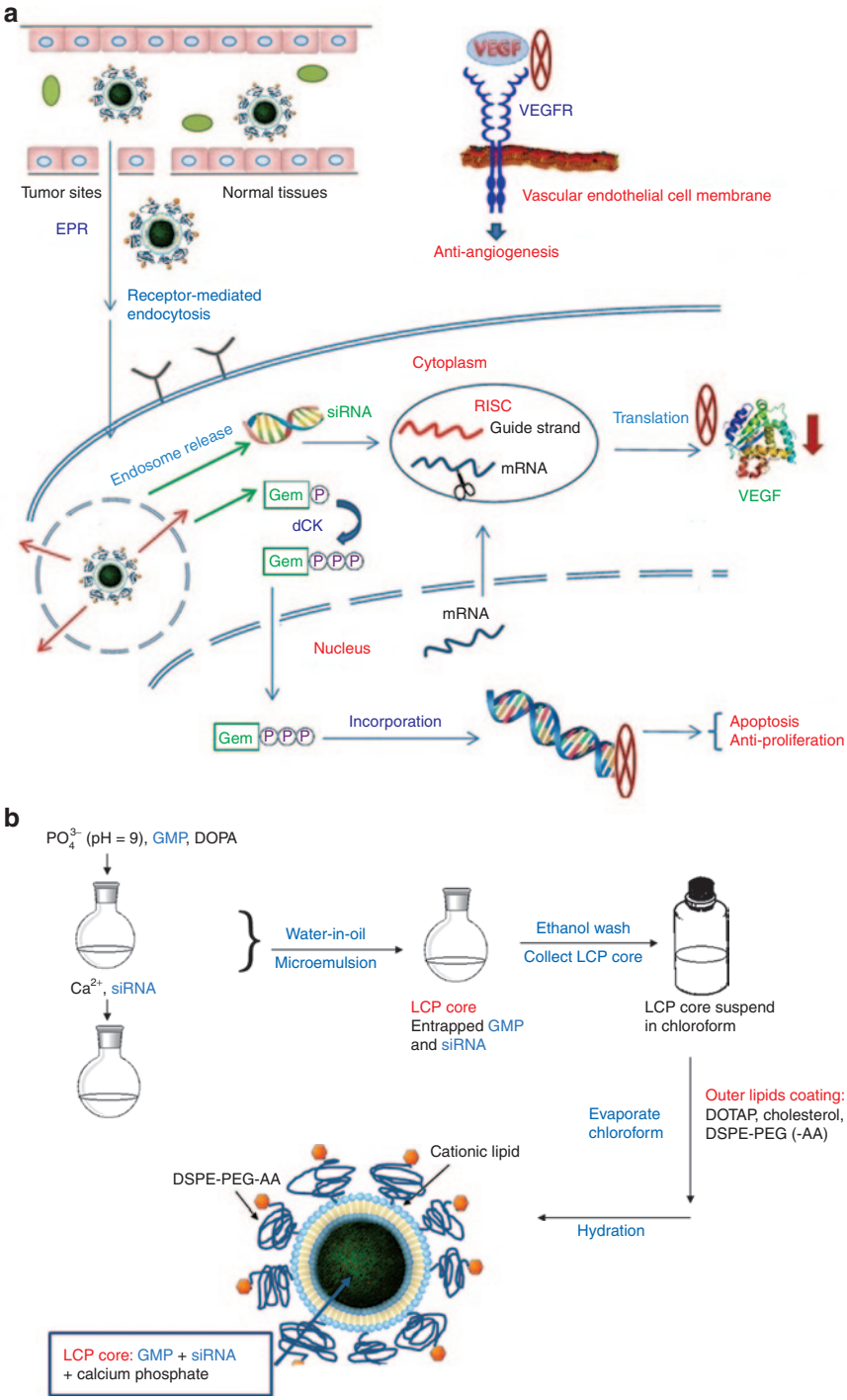

Figure 1 Schematic illustration of (a) the *in vivo* codelivery mechanism and (b) the preparation procedure of GMP- and/or VEGF siRNA–loaded LCP formulations. AA, anisamide; EPR, enhanced permeability and retention; GMP, gemcitabine monophosphate; LCP, lipid/calcium/phosphate.

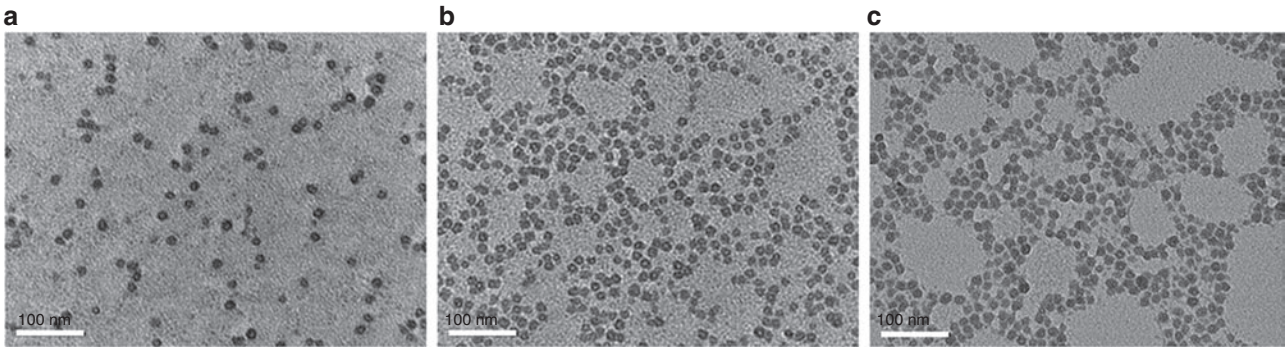

Figure 2 TEM pictures of (a) VEGF-LCPs, (b) GMP-LCPs, and (c) (GMP+VEGF)-LCPs. Scale bar = 100 nm. GMP, gemcitabine monophosphate; LCP, lipid/calcium/phosphate; VEGF, Vascular endothelial growth factor.

bilayer. The lipid membrane wrapping around the core is modified by grafting a high density of polyethylene glycol (PEG) chains, with a tethered targeting ligand AA. The preparation scheme of LCP is illustrated in **Figure 1b**.

The transmission electron microscope (TEM) photographs showed that all drug-loaded LCP-AAs had a spherical shape and were monodispersed, with a particle size of around 20 nm (**Figure 2**). The relatively small size of LCPs renders them better tumor penetration capability over large size nanoparticles.[11] The zeta potentials of VEGF-LCP-AA, GMP-LCP-AA, and (GMP+VEGF)-LCP-AA were 30.2 ± 14.1 mV, 3.4 ± 3.1 mV, and 10.0 ± 4.0 mV, respectively. The zeta potential of (CMP+Con)-LCP-AA was identical to the zeta potential of (GMP+VEGF)-LCP-AA. The encapsulation efficiency (EE%) of VEGF siRNA and GMP in LCP-AA was around 55 and 75%, respectively. The EE% of VEGF siRNA and GMP in coformulated LCP-AA was almost the same as that of the VEGF-LCP-AA or GMP-LCP-AA single formulation, which indicates that VEGF siRNA and GMP did not interfere with each other in the process of coprecipitation with calcium ions within the LCP core.

Drug-loaded LCPs induced VEGF downregulation and apoptosis *in vivo*

Human NSCLC H460 tumor–bearing mice were given three daily IV injections of different LCP formulations with a dose of 50.4 μmol/Kg GMP (19.5 mg/Kg GMP, or 13.2 mg/Kg in terms of Gem) and/or 0.2 mg/Kg VEGF siRNA. Twenty-four hours after the third injection, mice were killed and tumor lysates were prepared for western blot, and the RNAs in tumors were extracted for the RT-PCR measurement of VEGF mRNA levels. VEGF-VEGFR signaling in the endothelial cells of tumor blood vessels can be prevented by silencing VEGF. PARP is a nuclear protein that performs central roles in the repair of damaged DNA. Cleavage of PARP by caspases is considered to be a hallmark of apoptosis.[12] As shown in **Figure 3**, (GMP+VEGF)-LCP-AA showed significant knockdown of VEGF, and stimulated the overexpression of cleaved PARP. GMP-LCP-AA activated the cleaved PARP overexpression and had a partial effect on the VEGF expression level. VEGF-LCP-AA clearly reduced the VEGF expression, but had limited effect on PARP cleavage. Compared with the control, (CMP+Con)-LCP-AA had no measurable effect on the protein expression level of VEGF, and was not able to cleave PARP. Tumor

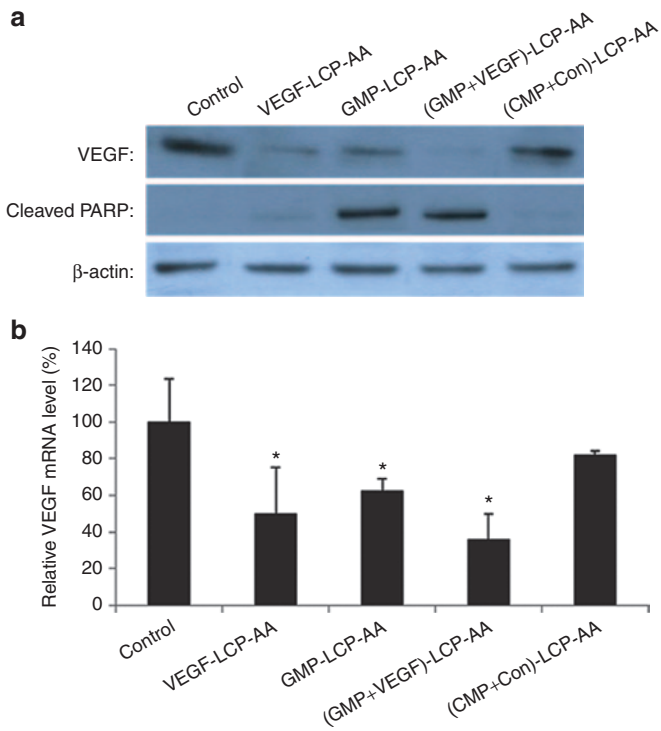

Figure 3 Western blot analysis and VEGF mRNA level after systemic treatments. H460 tumor–bearing mice were given three daily IV injections, and mice were killed 24 hours after the final injection. (**a**) Tumor lysates were prepared for western blot analysis. (**b**) Tumor VEGF mRNA levels in different treatment groups (n = 5) were measured by RT-PCR. Data are shown as mean ± SD. *P < 0.05 versus control. AA, anisamide; GMP, gemcitabine monophosphate; LCP, lipid/calcium/phosphate; VEGF, Vascular endothelial growth factor.

VEGF mRNA levels in different treatment groups (**Figure 3b**) coincided with the VEGF protein expression levels in the western blot analysis (**Figure 3a**).

Drug-loaded LCPs triggered caspase activation and tumor cell apoptosis *in vivo*

Caspases are proteolytic enzymes and play an important role in apoptosis as effector molecules. Among the caspase enzymes, caspase-3 and caspase-7 are especially important, and they are responsible for the proteolytic cleavage of a large number of substrates during apoptosis.[13] Twenty-four hours after three daily

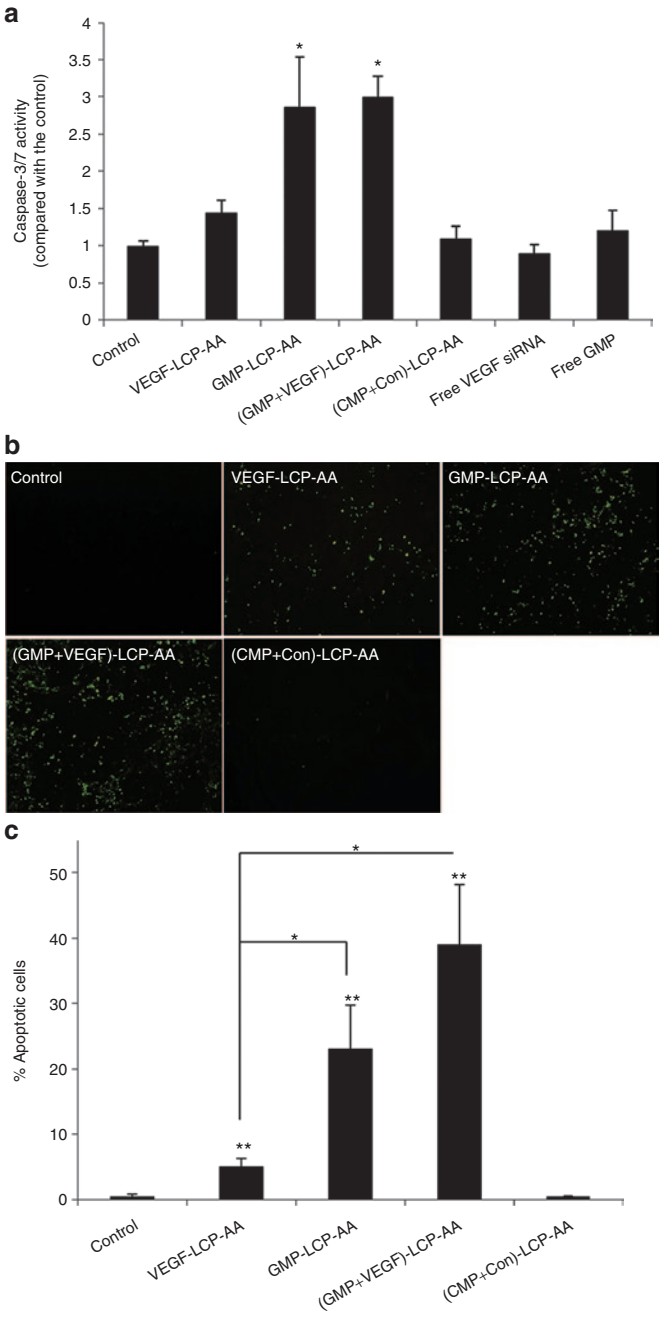

Figure 4 The caspase activation and induction of apoptosis after the systemic administration of different LCPs in H460 xenografts. (**a**) *In vivo* caspase-3/7 activity in tumors. **P* < 0.01, GMP-LCP-AA versus control, (GMP+VEGF)-LCP-AA versus control, GMP-LCP-AA versus VEGF-LCP-AA, and (GMP+VEGF)-LCP-AA versus VEGF-LCP-AA. (**b**) *In vivo* tumor apoptosis by TUNEL assay. (**c**) The percentage (%) of apoptotic cells in the TUNEL assay. ***P* < 0.005, VEGF-LCP-AA versus control, GMP-LCP-AA versus control, (GMP+VEGF)-LCP-AA versus control; **P* < 0.01, GMP-LCP-AA versus VEGF-LCP-AA, (GMP+VEGF)-LCP-AA versus VEGF-LCP-AA (*n* = 5 per group). AA, anisamide; GMP, gemcitabine monophosphate; LCP, lipid/calcium/phosphate; VEGF, Vascular endothelial growth factor.

IV injections, caspase-3/7 activity in H460 subcutaneous tumors was increased threefold in mice injected with (GMP+VEGF)-LCP-AA and GMP-LCP-AA and 1.5-fold in mice injected with VEGF-LCP-AA, as compared with the control (**Figure 4a**). (CMP+Con)-LCP-AA, free VEGF siRNA, and free GMP displayed little caspases elevation (**Figure 4a**). The results indicated that the LCPs greatly improved the *in vivo* delivery efficiency of VEGF siRNA and GMP, and the caspase activation was triggered mainly by GMP rather than VEGF siRNA.

We also measured the apoptotic induction in H460 subcutaneous tumor tissues using the TdT-mediated dUTP Nick-End Labeling (TUNEL) assay. Twenty-four hours after three daily IV injections, (GMP+VEGF)-LCP-AA triggered a dramatic killing effect, inducing 40% apoptotic cells in tumors. GMP-LCP-AA and VEGF-LCP-AA led to 22 and 5% apoptotic tumor cells, respectively. (CMP+Con)-LCP-AA did not elicit tumor cell apoptosis (**Figure 4b**). The tumor cell apoptotic induction of (GMP+VEGF)-LCP-AA was significantly higher than GMP-LCP-AA and VEGF-LCP-AA, indicating a profound therapeutic effect of the combined LCP. GMP-loaded LCPs were more potent than VEGF-loaded LCP in terms of tumor cell–killing effect.

Drug-loaded LCPs inhibited the formation of tumor vasculature

Next, we evaluated the effect of different LCP formulations on the formation of tumor vasculature on H460 subcutaneous tumor–bearing mice. We compared two treatment regimens: a frequent treatment schedule and an infrequent treatment schedule. The frequent treatment was characterized by daily IV injections over 3 consecutive days; the mice were killed 24 hours after the final injection. The infrequent treatment was characterized by IV injections given every other day over 8 days, totaling four injections. Mice treated with this regimen were killed 2 days after the final injection. **Figure 5** shows the results of staining CD31 antigen, an endothelial cell-specific surface marker. Control tumor showed thick, elongated, and disorganized layers of the vascular endothelium. (GMP+VEGF)-LCP-AA caused a significant reduction in tumor vasculature in both frequent and infrequent treatments, indicating an immediate and lasting effect of tumor angiogenesis inhibition. VEGF-LCP-AA dramatically shut down the tumor vasculature after infrequent treatment, but only displayed partial antiangiogenesis effects with sparsely dispersed microvessels after frequent treatments, indicating that VEGF-LCP-AA needs more time to effectively impair the tumor vasculature. It seems that GMP codelivered in the combined LCPs sensitized the tumor vasculature for antiangiogenesis therapy. Indeed, Gem can induce apoptosis in tumor-associated endothelial cells, leading to a decrease in microvessel density (MVD).[14,15] GMP-LCP-AA caused partial reduction of tumor vessel formation after multiple doses. (CMP+Con)-LCP-AA and free GMP had little effect on the alteration of the endothelial cells compared with the control. The quantitative MVD results were shown in **Figure 5b,d**.

Drug-loaded LCPs triggered tumor cell apoptosis and inhibited tumor cell proliferation *in vivo*

The H460 tumor–bearing mice were given IV injections of different LCP formulations every other day for a total of four injections. Two days after the final injection, the mice were killed and the tumors were sectioned for TUNEL assay, proliferating cell nuclear antigen (PCNA) immunohistochemistry and H&E stain. In the

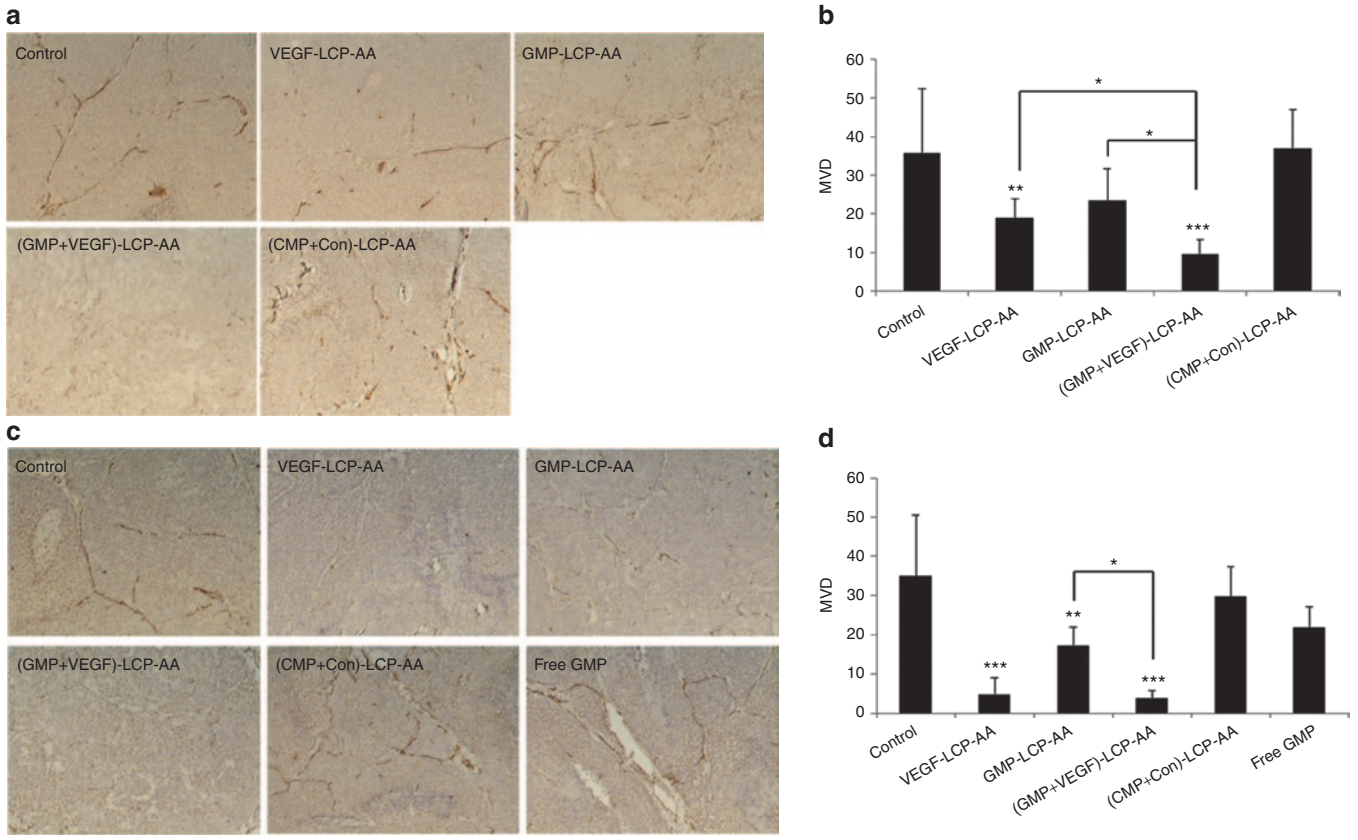

Figure 5 (**a**,**b**) CD31 immunohistochemistry staining of H460 xenograft tumors after frequent treatment and (**c**,**d**) infrequent treatment of different LCP formulations. (**b**) Statistics for frequent treatment: $*P < 0.05$, $**P < 0.005$ versus control, $***P < 0.00005$ versus control. (**d**) Statistics for infrequent treatment: $*P < 0.01$, $**P < 0.005$ versus control, $***P < 0.000001$ versus control. ($n = 5$ per group). GMP, gemcitabine monophosphate; LCP, lipid/calcium/phosphate; MVD, microvessel density; VEGF, Vascular endothelial growth factor.

TUNEL assay (**Figure 6a**), (GMP+VEGF)-LCP-AA elicited the most effective killing effects and triggered a significant amount (~30%) of apoptotic cells in the tumor, more potent than GMP-LCP-AA which induced 12% apoptotic cells. The results indicates antiangiogenesis-induced tumor cell starvation may augment the intrinsic cytotoxicity and duration of antitumor effects of the coformulated GMP.[16] Treatment with VEGF-LCP-AA was less efficient than with GMP-LCP-AA, only 3% of tumor cells underwent apoptosis. (CMP+Con)-LCP-AA and free GMP had limited ability to induce apoptosis in tumor cells.

We also evaluated the antiproliferation effect of different LCP formulations on H460 tumor–bearing mice. PCNA is expressed in the cell nuclei during DNA synthesis and can be used as a marker for cell proliferation. As shown in **Figure 6c**, (GMP+VEGF)-LCP-AA significantly decreased the number of PCNA positive cells in H460 xenograft tumors. VEGF-LCP-AA and GMP-LCP-AA also caused reductions in the proliferation of tumor cells. The antiproliferation effect of VEGF-LCP-AA indicates that VEGF not only acts as an endothelial-specific growth factor, it can also promote proliferation of tumor cells.[17] However, (CMP+Con)-LCP-AA and free GMP showed little antiproliferative effect. From this infrequent dosing treatment, we had observed additive tumor cell–killing and antiproliferation effects of (GMP+VEGF)-LCP-AA compared with the monotherapy of GMP-LCP-AA or VEGF-LCP-AA.

Drug-loaded LCPs inhibited mitotic figures in tumors

As shown in the H&E stain (**Figure 6e**), after infrequent treatment in H460 tumor–bearing mice, the control tumor had many mitotic figures, showing a high mitotic activity of tumor cells. Some typical mitotic figures were shown by arrows in blue. The chromosomes of the mitotic figures are visible as tangled, dark-staining threads or spots. Counting mitotic figures serves as a tool for differentiating benign tumors from malignant ones.[18] The control tumor displayed various cell morphologies with dark clumped chromatin, indicating uncontrollable tumor growth and poor differentiation, otherwise known as malignancy. Cellular and nuclear features also correlated with proliferative activity, with untreated tumors exhibiting marked anisocytosis and anisokaryosis (variation in cell and nuclear size), polyploidy, and open vesicular nuclei with dispersed chromatin and prominent nucleoli. Tumors that were treated with (GMP+VEGF)-LCP-AA experienced a dramatic decrease in mitotic figures and exhibited more basophilic and uniform nuclei. However, some chromosome condensation remained due to the cytotoxicity induced by the combined therapy. The decrease in mitotic figures supported the aforementioned PCNA staining, indicating the antiproliferation effects of (GMP+VEGF)-LCP-AA partially results from the inhibition of cell mitosis in tumors. VEGF-LCP-AA and GMP-LCP-AA also triggered a decrease in mitotic figures compared with the control. The mitotic figures of tumors in each group are shown quantitatively in **Figure 6f**.

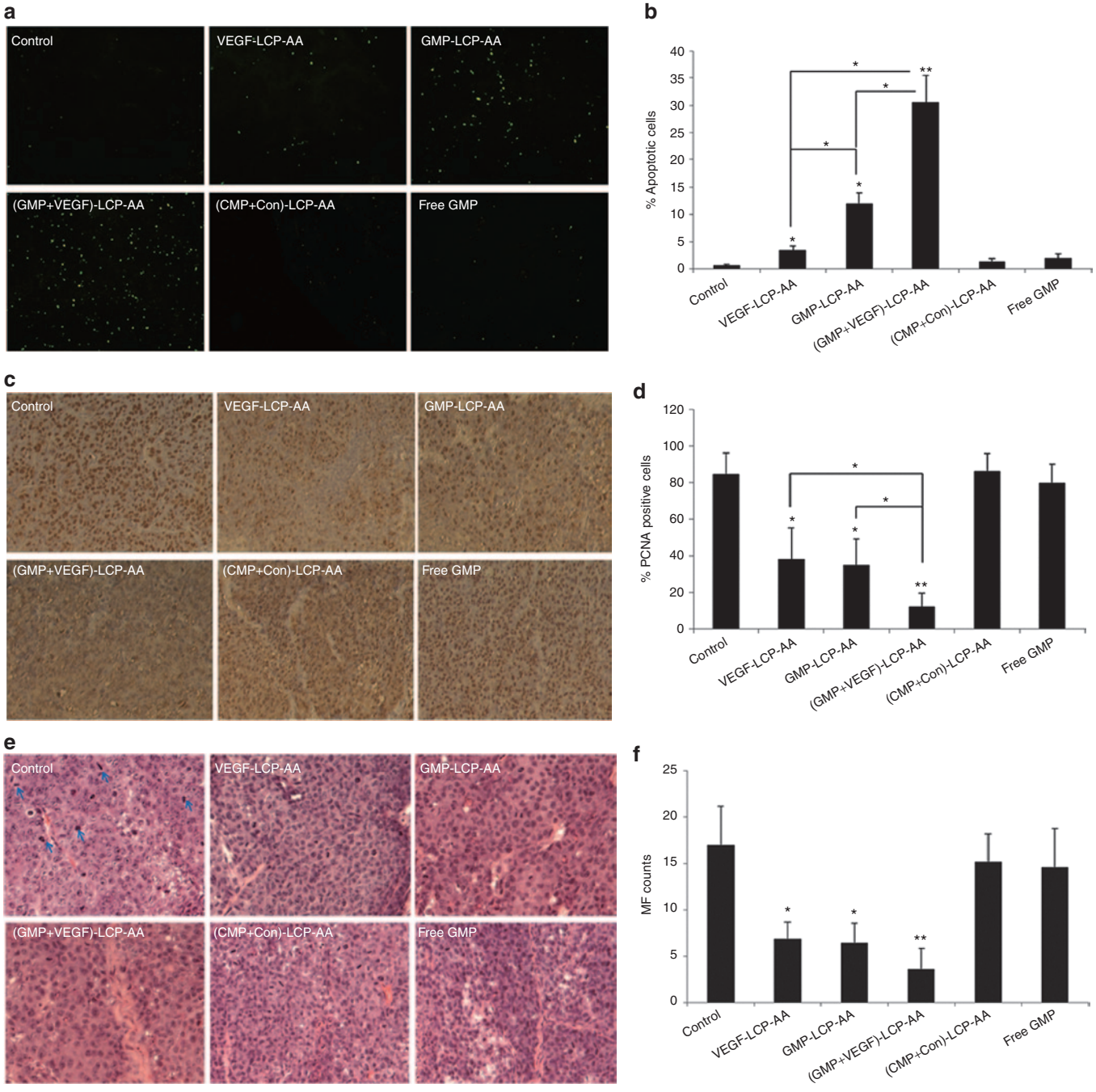

Figure 6 VEGF-LCP-AA, GMP-LCP-AA, (GMP+VEGF)-LCP-AA, (CMP+Con)-LCP-AA and free GMP were administered intravenously every other day for total four injections. Two days after the last injection, H460 tumor–bearing mice were killed and tumor tissues were sectioned for (**a**,**b**) TUNEL assay and (**c**,**d**) PCNA immunohistochemistry. (**e**) Mitotic figures (MF) in tumors were evaluated by H&E stain. (**b**) Statistics of the TUNEL assay in H460 xenografts: *$P < 0.005$, VEGF-LCP-AA versus control, GMP-LCP-AA versus control, VEGF-LCP-AA versus GMP-LCP-AA, VEGF-LCP-AA versus (GMP+VEGF)-LCP-AA, GMP-LCP-AA versus (GMP+VEGF)-LCP-AA; **$P < 0.001$, (GMP+VEGF)-LCP-AA versus control. (**d**) Statistics of the PCNA immunohistochemistry in H460 xenografts: *$P < 0.05$, VEGF-LCP-AA versus control, GMP-LCP-AA versus control, (GMP+VEGF)-LCP-AA versus VEGF-LCP-AA, (GMP+VEGF)-LCP-AA versus GMP-LCP-AA; **$P < 0.01$, (GMP+VEGF)-LCP-AA versus control. (**f**) Statistics of mitotic figures in tumors: *$P < 0.001$, VEGF-LCP-AA versus control, GMP-LCP-AA versus control; **$P < 0.0001$, (GMP+VEGF)-LCP-AA versus control. ($n = 5$ per group). AA, anisamide; CMP, Cytidine monophosphate; GMP, gemcitabine monophosphate; LCP, lipid/calcium/phosphate; VEGF, Vascular endothelial growth factor.

Tumor growth inhibition

The tumor growth inhibition was evaluated in nude mice bearing H460 subcutaneous tumors. Mice were treated every other day for a total of four IV injections with a dose of 50.4 μmol/Kg GMP and/or 0.2 mg/Kg VEGF siRNA. As shown in **Figure 7**, (GMP+VEGF)-LCP-AA exhibited the most effective tumor growth inhibition; growth was almost completely arrested during the combined therapeutic regimen. GMP-LCP-AA also suppressed tumor growth effectively, but not as potently as the combined nanoparticle treatment. Antiangiogenic monotherapy

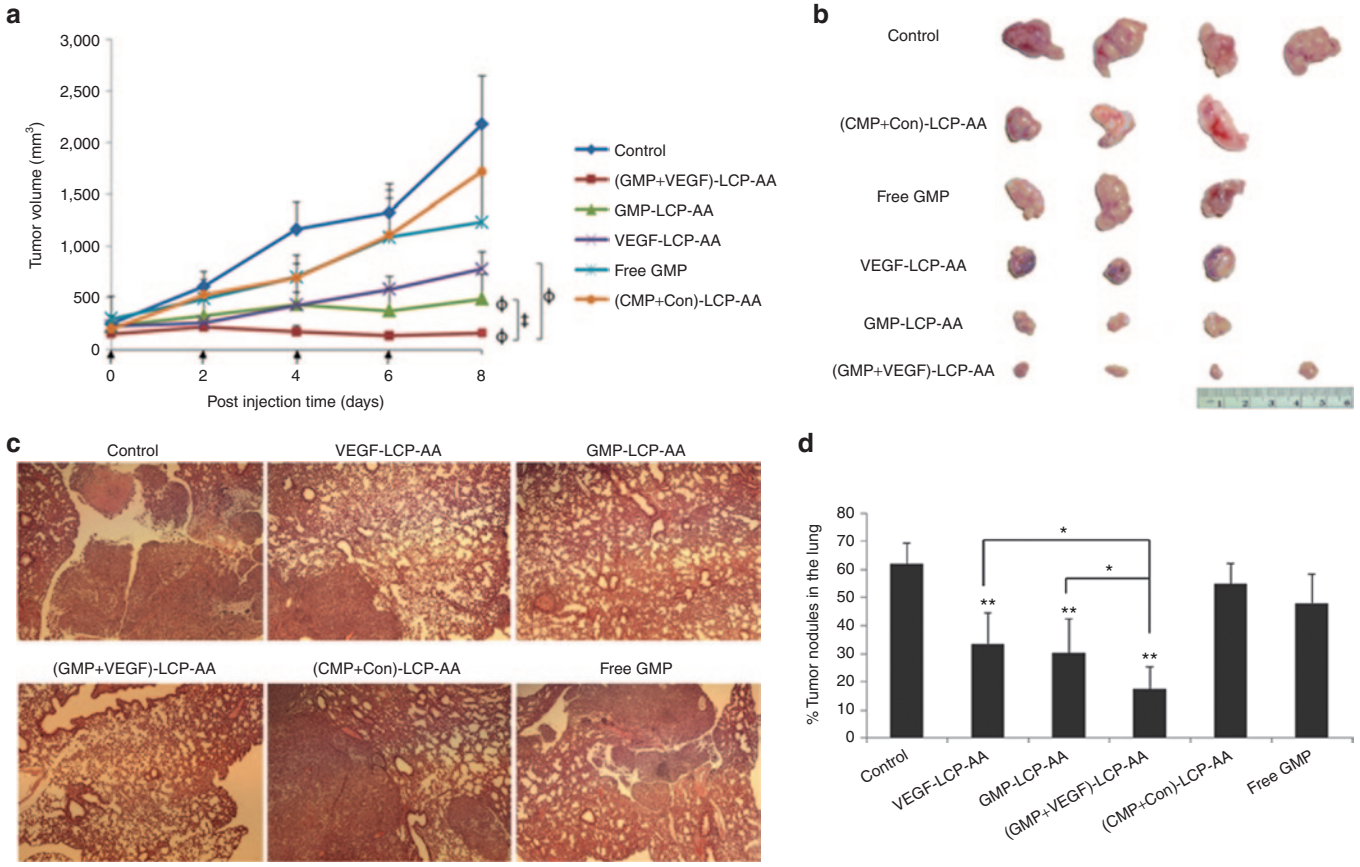

Figure 7 Tumor growth inhibition in subcutaneous and orthotopic tumor models of NSCLC. (**a**) Tumor growth inhibition effects of different LCP formulations on H460 tumor–bearing mice. VEGF-LCP-AA, GMP-LCP-AA, (GMP+VEGF)-LCP-AA, (CMP+Con)-LCP-AA, and free GMP were administered intravenously every other day for total four injections. Tumor volumes were measured every other day. Data are mean ± S.D. (n = 6–7 per group) Statistics are as follows: *P < 0.01, VEGF-LCP-AA versus control; $^{\phi}P$ < 0.001, GMP-LCP-AA versus control, (GMP+VEGF)-LCP-AA versus control, (GMP+VEGF)-LCP-AA versus VEGF-LCP-AA; $^{\ddagger}P$ < 0.05, (GMP+VEGF)-LCP-AA versus GMP-LCP-AA.*P < 0.01, (GMP+VEGF)-LCP-AA versus (CMP+Con)-LCP-AA. (**b**) Visual observations of the H460 tumor sizes in each treatment group at the end time point. (**c**) Representative histopathology examination (H&E staining) of orthotopic lung tumors after LCP treatments. (**d**) Percentages (%) tumor nodules in the lung in the orthotopic tumor model. *P < 0.05, **P < 0.005 versus control. (n = 6 per group). AA, anisamide; CMP, Cytidine monophosphate; GMP, gemcitabine monophosphate; LCP, lipid/calcium/phosphate; VEGF, Vascular endothelial growth factor.

with VEGF-LCP-AA was not sufficient to obtain long-term tumor suppression. VEGF-LCP-AA stabilized the tumor growth at early stages of treatment, but unfortunately, was associated with insufficient anticancer activity and tumor progression at later stages. The (CMP+Con)-LCP-AA and free GMP had little effect on tumor growth inhibition compared with the control. At the treatment end point, representative tumors in each treatment group were harvested (**Figure 7b**) for visual comparison. Tumors treated with (GMP+VEGF)-LCP-AA were smaller than tumors in other treatment groups. Thus, the combined treatment with (GMP+VEGF)-LCP-AA was significantly more effective than treatment with GMP-LCP-AA and VEGF-LCP-AA individually.

We further tested the combination therapy in murine orthotopic models of human NSCLC that closely recapitulate the clinical pattern and progression of lung cancer in humans using A549 NSCLC cell lines. Increased visible lung surface nodules were indicative of increased tumor burden in orthotropic tumor model. As shown in the H&E histopathology analysis (**Figure 7c**), the lung of untreated mice revealed some neoplastic nodules scattering in the parenchyma of the lung lobe and some tumor mass adhering to the periphery of the lung or attached in between the airway. Some orthotopic tumor nodules displayed a massive and contiguous invasion into the surrounding alveolar wall and lung alveoli, and necrotic zones can be observed in the central region of some tumors. Comparing with the untreated mice, mice treated with VEGF-LCP-AA and GMP-LCP-AA displayed a 50% reduction in size of orthotopically implanted lung tumors; mice treated with (GMP+VEGF)-LCP-AA displayed a 70% reduction in size of the orthotopic lung tumors.

(GMP+VEGF)-LCP-AA reduced the *in vivo* toxicity

To test whether GMP and VEGF siRNA–loaded LCPs would induce *in vivo* toxicity, especially hepatic and renal dysfunction after frequent multiple dosing, CD-1 mice were given three daily IV injections. Twenty-four hours after the final injection, blood samples were obtained for hematological analysis and histopathology of different organs were evaluated by H&E stain. As shown in **Table 1**, within the normal range, VEGF-LCP-AA induced a relatively high level of blood urine nitrogen. GMP-LCP-AA led to higher aspartate aminotransferase and alanine aminotransferase compared with the

Table 1 Serum levels of BUN, creatinine, AST, and ALT after three daily IV injections in H460 xenograft model

	BUN mg/dl	Creatinine mg/dl	AST U/l	ALT U/l
Control	15.0 ± 3.0	0.4 ± 0.1	129.5 ± 2.5	45.0 ± 1.0
VEGF-LCP-AA	33.0 ± 1.0	0.4	158.5 ± 3.5	30.5 ± 8.5
GMP-LCP-AA	11.0 ± 1.0	0.4 ± 0.1	371.5 ± 31.5	81.0 ± 15.0
(GMP+VEGF)-LCP-AA	15.0 ± 1.0	0.5	213 ± 95.1	35.0 ± 10.0
Reference range	8–33	0.2–0.9	54–298	17–132

Data are mean ± SD (n = 5 per group).
AA, anisamide; ALT, alanine aminotransferase; AST, aspartate aminotransferase; BUN, blood urine nitrogen; GMP, gemcitabine monophosphate; LCP, lipid/calcium/phosphate; VEGF, Vascular endothelial growth factor.

control. However, treatment with (GMP+VEGF)-LCP-AA alleviated the elevations of blood urine nitrogen, aspartate aminotransferase, and alanine aminotransferase and kept the parameters of kidney and liver functions within the normal range. The administration of chemotherapy to patients with liver impairment may result in complicated safety issues, a treatment regimen using the nanoparticles formulated with both GMP and VEGF siRNA can help alleviate the potential liver toxicity as well as enhance the therapeutic response, compared with treatment with a single agent. From the H&E-stained tissue sections of heart, liver, spleen, lung, and kidney (**Supplementary Figure S1**), there were no noticeable histological changes between the control and (GMP+VEGF)-LCP-AA treatment group, which showed no evidence of organ toxicity. In addition, at the therapeutic dose, no significant immune response was elicited after bolus IV administration, as evidenced by the production of serum cytokines, including interleukin (IL)-6, IL-12, tumor necrosis factor (TNF)-α, and interferon (IFN)-γ (**Figure 8**). Taken together, LCP formulations encapsulating chemotherapeutic agents and therapeutic siRNAs show safety and low immunogenicity *in vivo*.

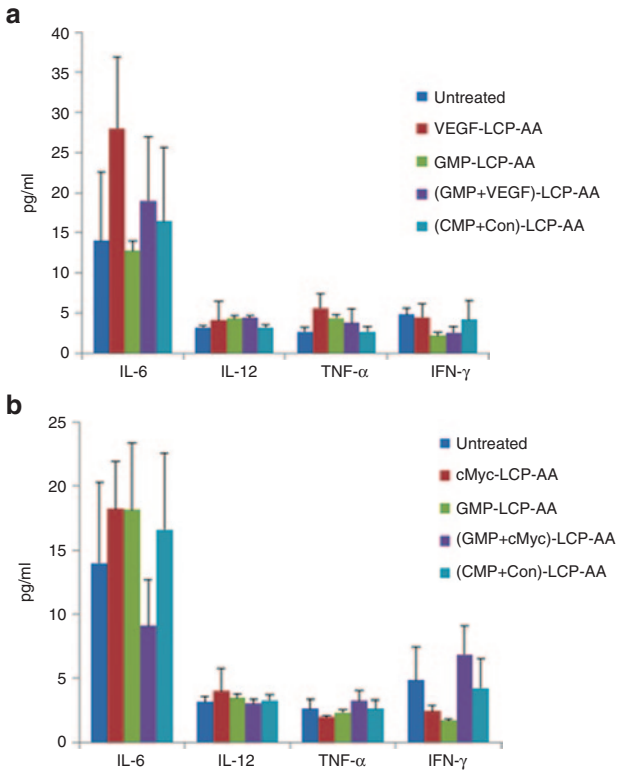

Figure 8 Immunotoxicity analysis on normal mice. Mouse serum was collected (**a**) 4 hours and (**b**) 24 hours after bolus IV administration of different LCPs at the therapeutic dose. Interleukin (IL)-6, IL-12, tumor necrosis factor (TNF)-α, and interferon (IFN)-γ were measured by ELISA. Data = mean ± SD (n = 5 per group). AA, anisamide; CMP, Cytidine monophosphate; GMP, gemcitabine monophosphate; LCP, lipid/calcium/phosphate; VEGF, Vascular endothelial growth factor.

DISCUSSION

In this study, we report a novel systemic delivery platform consisting of the coformulation of nucleic acid molecules and phosphorylated, small-molecule drugs in a single LCP nanoparticle. GMP and VEGF siRNA were coformulated using LCP nanotechnology to target two therapeutic pathways of an aggressive human cancer malignancy (*i.e.*, NSCLC). Specifically, our delivery system aimed to induce apoptosis though GMP chemotherapy and to shut down the tumor neovasculature by blocking the VEGF-VEGFR signaling cascade with VEGF RNAi.

Phosphate groups on the molecules can interact with calcium in a microemulsion, enabling the encapsulation of GMP and VEGF siRNA in the nanoparticle system containing a calcium phosphate precipitate (CaP) core (*i.e.*, LCP). A lipid bilayer surrounds the CaP core to allow a high density of DSPE-PEG to be grafted onto the surface. The surface modification with PEG helps shield the cationic charge of the lipid bilayer and may minimize the interaction with circulating blood components to prolong circulation time of the particle. The prolonged circulation half-life is a prerequisite for enhanced tumor targeting and increases the probability that the LCPs will encounter the "leaky" tumor vasculature and be exposed to the enhanced permeability and retention effect.[19] The LCP's high density PEG and small size allow it to evade the reticuloendothelial system surveillance, which promote tumor accumulation (**Supplementary Figure S2**) and decrease toxicity in the liver and kidney. With AA as a tumor-specific targeting ligand, LCPs can be more effectively taken up into tumor cells via sigma-receptor–mediated endocytosis. In addition, the design of the CaP core also promotes endosomal release of the cargo while preventing lysosomal degradation of the entrapped VEGF siRNA and GMP. When LCPs are delivered into acidic endosomes, the CaP core of the LCPs rapidly dissolves to increase the osmotic pressure in the endosome, eventually bursting the endosomes and enabling the entrapped GMP and VEGF siRNA to escape (**Figure 1a**).[20] The cationic lipid, DOTAP, surrounding the LCP core may also promote the release of the entrapped cargo by destabilizing the anionic endosome membrane.[21]

Loading Gem derivatives in LCPs can potentially avoid drug efflux proteins (e.g., MRP, BCRP) and the deficiency of cellular uptake caused by the mutations of nucleoside transporters (e.g., ENT1, ENT2, CNT1, CNT3) in the cell membrane. In our previous study, we have validated that the nucleotide analogue Gem triphosphate (GTP)–loaded LCP nanoparticle showed significant antitumor efficacy on lung and pancreatic xenograft models.[22] We later found that comparing with GTP which was synthesized in an big organic salt form, GMP (disodium salt form) gave us higher

EE% and drug loading, such that similar antitumor efficacy was attained. So, GMP was used in the current study. The monophosphate modification on GMP allows it to bypass the first rate-limiting phosphorylation step, greatly increasing the conversion rate to biologically active Gem triphosphate derivatives. On the other hand, the downregulation of VEGF expression in tumors leads to blockage of the sequential survival signaling initiated by dimerization and autophosphorylation of VEGFR molecules. Blocking VEGF/VEGFR signaling by downregulating VEGF potently inhibits aberrant angiogenesis (**Figure 1a**). In addition, LCPs can potentially protect VEGF siRNA and GMP from enzymatic degradation (*i.e.,* nuclease and deoxycytidine deaminase, respectively) and renal clearance *in vivo*.

This study indicates that combining antiangiogenesis treatment with chemotherapy through systemic administrations of LCP nanoparticles containing both VEGF siRNA and phosphorylated Gem results in an additive antitumor effect. The codelivered VEGF siRNA that can damage existing blood vessels in tumors might influence response to the concurrent chemotherapy. Combination therapies are most likely successful because damaging the established tumor endothelium has been shown to increase vessel permeability and facilitate the delivery of subsequently administered LCPs and the coformulated GMP.[23] The significant knockdown of the proangiogenic protein, VEGF, caused by the systemic administrations of (GMP+VEGF)-LCP-AA illustrates that this treatment regime can lead to decreased tumor angiogenesis (**Figure 3**). Furthermore, MVD is reduced through the reduction of VEGF/VEGFR interactions and the resulting signaling cascades, as indicated by the expression of CD31 antigen in vascular endothelial cells (**Figure 5**). These effects of (GMP+VEGF)-LCP-AA modify the tumor microenvironment to potentiate the delivery of the chemodrug. GMP entrapped in the combined LCP subsequently inhibits the prosurvival program as evidenced by elevated PARP cleavage and caspase activation (**Figures 3a** and **4a**), significant induction of tumor cell apoptosis and reduction of tumor cell proliferation (**Figures 4b** and **6**).

The advantages of nanoparticles containing multiple drugs are that they can offer the unique features of vehicle uniformity, ratiometric drug loading and temporal drug release, while maintaining the ability to unify the pharmacokinetics of different drugs they encapsulate. These nanoparticles are thereby able to simultaneously deliver multiple gene- and/or chemotherapeutic agents to the target site.[24] We have done some preliminary work on the comparison of (GMP+VEGF)-LCP-AA and the coadministered mixture of GMP-LCP-AA and VEGF-LCP-AA on the antitumor therapeutic response. The results indicated the combined (GMP+VEGF)-LCP-AA had more potency in inducing cell-killing effects compared with the administration of separate LCPs loaded with each individual agent (data not shown). The pharmacokinetic profiles and the therapeutic effects of the drug loading ratio are now under investigation. The strategy of coformulating multiple gene therapeutics and phosphorylated chemodrugs in a single vector via LCP nanotechnology is expected to lead to superior therapeutic improvement in many human diseases, and to modulate multiple therapeutic pathways simultaneously.

MATERIALS AND METHODS

Materials. GMP disodium salt was synthesized by HDH Pharma (Research Triangle Park, NC). VEGF siRNA (target sequence: 5′-ACC UCA CCA AGG CCA GCA C-3′) and control siRNA (target sequence: 5′-AAU UCU CCG AAC GUG UCA CGU-3′) were synthesized by Sigma-Aldrich (St Louis, MO). 1,2-Dioleoyl-3-trimethylammonium-propane chloride salt (DOTAP), dioleoylphosphatydic acid (DOPA), and 1,2-distearoryl-sn-glycero-3-phosphoethanolamine-N-[methoxy(polyethylene glycol-2000) ammonium salt (DSPE-PEG_{2000}) were purchased from Avanti Polar Lipids (Alabaster, AL). DSPE-PEG-AA was synthesized in our lab as described previously.[25] DeadEnd Fluorometric TUNEL assay kits and Apo-ONE Homogeneous Caspase-3/7 assay substrates were obtained from Promega (Madison, WI). Other chemicals were obtained from Sigma-Aldrich.

Cell culture. H460 human NSCLC cells, originally obtained from American Type Culture Collection (ATCC, Manassas, VA), were cultured in RPMI-1640 medium (Invitrogen, Carlsbad, CA) supplemented with 10% fetal bovine serum, 100 U/ml penicillin, and 100 µg/ml streptomycin (Invitrogen). Cells were cultivated in a humidified incubator at 37 °C and 5% CO_2. Cells were harvested with 0.05% trypsin-EDTA before subculture.

Experimental animals. Female nude mice 6–8 weeks of age were used in all studies. To establish the xenograft models, 5×10^6 H460 cells in 100 µl of phosphate-buffered saline were injected subcutaneously into the right flank of mice. Experiments were performed 11 days after the tumor implantation. For the orthotopic model, nude mice were anesthetized and a 0.5 cm incision was made after skin disinfection. 5×10^6 A549 cells in 40 µl of Matrigel-PBS medium (v/v = 1:1) were injected via a 28-gauge needle about 2 cm up from the bottom of the ribcage via the left dorsal side of nude mice. The incision was closed with a surgery clamp. All animals were maintained at a surgical plane of anesthesia during the procedure. The mice in control group were untreated mice with no injections. All work performed on animals was approved by the Institutional Animal Care and Use Committee at University of North Carolina at Chapel Hill.

Preparation of VEGF-LCP-AA, GMP-LCP-AA, and (GMP+VEGF)-LCP-AA. LCP cores were prepared using water-in-oil microemulsions, with the oil phase containing cyclohexane/Igepal CO-520 solution (71/29, v/v).[26] To prepare the VEGF-LCP cores, 48 µg VEGF siRNA was mixed with 600 µl 2.5 mol/l $CaCl_2$ and added into 20 ml of oil phase, where the other emulsion contained 600 µl 12.5 mmol/l Na_2HPO_4 (pH = 9.0). The GMP-LCP core was formulated using 180 µl of 60 mmol/l GMP mixed with 12.5 mmol/l Na_2HPO_4 (pH = 9.0) (final concentration) to reach a total volume of 600 µl. This solution was then added into 20 ml of oil phase. A 600 µl 2.5 mol/l $CaCl_2$ was added to a separate the 20 ml oil phase. To prepare the (GMP+VEGF)-LCP core, the phosphate phase met the same specifications outlined in the preparation of the GMP-LCP core. The calcium phase contained 600 µl of 2.5 mol/l $CaCl_2$ mixed with 48 µg of VEGF siRNA. A 400 µl of 20 mmol/l DOPA in chloroform was added to the phosphate phase of the GMP-LCP and (GMP+VEGF)-LCP, whereas only 200 µl of 20 mmol/l DOPA was added to the phosphate phase during the preparation of the VEGF-LCP.

The two separate microemulsions were then mixed. After stirring for 5 minutes, another 400 µl of 20 mmol/l DOPA was added into the emulsion of GMP-LCP and (GMP+VEGF)-LCP; for VEGF-LCP, 200 µl of 20 mmol/l DOPA was added. The emulsion was allowed to continually stir for another 20 minutes before 40 ml of absolute ethanol was added. The ethanol emulsion mixture was centrifuged at 10,000*g* for 15 minutes to pellet the LCP core and the supernatant was then discarded. The LCP core was washed twice with absolute ethanol and dried under N_2. The LCP core pellets were suspended in 2 ml chloroform and stored in a glass vial at −20 °C for further use.

To prepare the final VEGF-LCP-AA, GMP-LCP-AA, and (GMP+VEGF)-LCP-AA with outer lipid outing, 330 µl LCP core in chloroform was mixed with 38.7 µl of 10 mg/ml Cholesterol, 28 µl of

25 mg/ml DOTAP, 76.8 μl of 25 mg/ml DSPE-PEG, and 19.2 μl of 25 mg/ml DSPE-PEG-AA. After evaporating the chloroform, the residual lipids were dissolved in 30 μl THF followed by 50 μl absolute ethanol, and then suspended in 160 μl water. After brief sonication, the solution was dialyzed in distilled water to remove the THF and ethanol. The preparation procedure of (CMP+Con)-LCP-AA was identical to that of (GMP+VEGF)-LCP-AA, except that GMP and VEGF siRNA were replaced by equal molar amount of CMP and control siRNA.

Characterization of VEGF-LCP-AA, GMP-LCP-AA, and (GMP+VEGF)-LCP-AA. The particle size and zeta potential of LCPs were determined by dynamic light scattering using a Malvern ZetaSizer Nano series (Westborough, MA). The EE% of GMP or siRNA was measured after lysing the LCPs with a THF/1 mol/l HCl (v/v = 70/30) solution. GMP EE% was measured using a UV spectrophotometer (Beckman Coulter, Brea, CA; DU 800 spectrophotometer) at a wavelength of 275 nm. The EE% of siRNA was measured by mixing a small amount of Texas-red–labeled siRNA with VEGF siRNA in LCP cores, and the fluorescence intensity of Texas-red was detected at the wavelength of Ex = 589 nm and Em = 615 nm. TEM images of LCP formulations were acquired through the use of JEOL 100CX II TEM (Tokyo, Japan). Briefly, 4 μl of LCP solution was dropped onto a 300 mesh carbon coated copper grid (Ted Pella, Redding, CA) for 2 minutes. Excess fluid was then removed with filter paper, and the copper grid was dried before observation using the TEM.[27]

Western blot and RT-PCR analysis. Twenty-four hours after the third injection, H460 tumor–bearing mice were killed and tumor lysates were prepared with radioimmunoprecipitation assay buffer, supplemented with a protease inhibitor cocktail (Promega). Protein concentrations were determined using a BCA assay kit (Pierce Biotechnology, Rockford, IL) following the manufacturer's recommendations. A 40 μg of protein per lane was separated by 4–12% SDS-PAGE electrophoresis (Invitrogen) before being transferred into polyvinylidenedifluoride membranes. The membranes were blocked for 1 hour with 5% silk milk at room temperature and then incubated with rabbit polyclonal VEGF antibody and mouse monoclonal poly(ADP-ribose) polymerase-1 (PARP-1) antibody (1:500 dilution; Santa Cruz Biotechnology) overnight at 4 °C. β-actin antibodies (1:4,000 dilution; Santa Cruz Biotechnology) served as the loading control. The membranes were washed three times and then incubated with secondary antibodies (1:4,000 dilution; Santa Cruz Biotechnology) at room temperature for 1 hour. Finally, the membranes were washed four times and developed by an enhanced chemiluminescence system according to the manufacturer's instructions (Thermo Scientific, Milford, MA).

RNAs in tumors were extracted with an RNeasy Mini Kit (Qiagen, Valencia, CA). The PCR primers and their fluorogenic probes for the target genes were designed by using the computer program Primer Express (PE Biosystems, Foster City, CA). The primer sequences for human VEGF were: forward, 5′-TCC AAC ATC ACC ATG CAG ATT-3′; reverse, 5′-GCA TTC ACA TTT GTT GTG CTG T-3′. The primer sequences for human β-action were: forward, 5′-GGT CAT CAC CAT TGG CAA TG-3′; reverse, 5′-TAG TTT CGT GGA TGC CAC AG-3′. A reporter dye (FAM for the target RNA and TET for the β-action control) of each fluorescent probe was covalently attached at its 5′ end and a quencher dye (TAMRA) was attached at its 3′ end. The probes were purified in the PolyPak II cartridge (Glen Research, Sterling, VA) following the manufacturer's instructions. RT-PCR amplifications were performed in a 96-well plate in the ABI Prism 7700 sequence detector system in a total volume of 30 μl, including 10 μl RNA sample and 20 μl of a reaction mixture made by following the manufacturer's instructions (PE Biosystems). Each RT-PCR amplification was performed in duplicate: 30 minutes at 48 °C for the RT reaction, then 10 minutes at 94 °C, followed by a total of 40 temperature cycles (15 seconds at 94 °C and 1 minutes at 60 °C).[28] During the amplification, the fluorescence of FAM (or TET), TAMRA, and ROX (a passive reference dye) was measured by the 7700 sequence detector in each well of the 96-well plate. The numbers of copies of the PCR template in the starting sample were calculated by using the Sequence Detector Software incorporated in the ABI Prism 7700 Sequence Detector System (Applied Biosystems, Foster City, CA).[28]

Caspase activation. Twenty-four hours after three daily IV injections, 40 μg protein of each tumor lysate was used to detect caspase-3/7 activity in tumors according to the manufacturer's instructions (Invitrogen, New York, NY). Briefly, 25 μl sample solution containing 40 μg of protein was added to a 96-well plate, and 25 μl caspase-3/7 reagent was added to each sample well. The contents of the wells were gently mixed at 400 rpm for at least 1 hour at room temperature. Their fluorescence was measured using a microplate reader at a wavelength of Ex = 485 nm and Em = 535 nm. The fluorescence intensity of treatment groups was normalized to that of the control group to indicate the extent of caspase activation.

TUNEL assay. After predetermined dosing schedule, H460 tumor–bearing mice were killed and tumors were fixed in 10% formalin for 24 hours before embedded in paraffin and sectioned at a thickness of 5 μm. The TUNEL staining was performed as recommended by the manufacturer (Promega). Then DAPI mounting medium was dropped on the sections for nucleus staining. Images of TUNEL-stained tumor sections were captured with a fluorescence microscope (Nikon, Tokyo, Japan). The percentage of apoptotic cells was obtained by dividing the number of apoptotic cells (TUNEL positive cells shown as green dots) from the number of total cells (blue nuclei stained by DAPI, data not shown) in each microscopic field, and 10 representative microscopic fields were randomly selected in each treatment group for this analysis.

Immunohistochemistry. Paraffin-embedded tumor sections were obtained as mentioned above. The CD31 (1:50 dilution, Abcam, Cambridge, MA) and PCNA (1:200 dilution, Santa Cruz Biotechnology) immunohistochemistry was performed using the HRP/DAB detection IHC kit as recommended by the manufacturer (Abcam). Immunostaining images were observed under a light microscope (Nikon). The percentage of proliferation cells was obtained by dividing the number of PCNA positive cells (shown as brown dots) from the number of total cells (blue nuclei stained by hematoxylin) in each microscopic field. MVD was evaluated by counting CD31 positive staining vessels in each microscopic field. At least 10 representative microscopic fields were randomly selected in each treatment group for counting.

Tumor growth inhibition. Tumor growth inhibition of the nanoparticles system was evaluated in an H460 subcutaneous xenograft mouse model. When the tumor volumes reached about 150–200 mm^3, the mice were randomly assigned into six treatment groups (n = 6–7), and intravenously injected different LCPs, including VEGF-LCP-AA, GMP-LCP-AA, (GMP+VEGF)-LCP-AA, (CMP+Con)-LCP-AA, and free GMP. The IV injections were performed every other day for a total of four injections with a dose of 50.4 μmol/Kg GMP and/or 0.2 mg/Kg VEGF siRNA. Tumor sizes were measured every other day with calipers across their two perpendicular diameters, and the tumor volume was calculated using the following formula: $V = 0.5 \times (W^2 \times L)$, where V = tumor volume, W = the smaller perpendicular diameter and L = the larger perpendicular diameter. Two days after the final injection, the mice were killed and the tumors were stripped off. Some tumors were fixed in 10% formalin and cut into paraffin-embedded tissue sections for TUNEL assay, immunohistochemistry analysis and an H&E stain. Other tumors were arranged and the photographs of tumors were taken as a visual comparison of the representative tumor sizes in each treatment group.

Four weeks after the orthotopic lung tumor implantation, mice were randomly assigned into 6 treatment groups (n = 6), and intravenously injected VEGF-LCP-AA, GMP-LCP-AA, (GMP+VEGF)-LCP-AA, (CMP+Con)-LCP-AA, and free GMP twice per week (once every 3 days) over 3 weeks, with a dose of 50.4 μmol/Kg GMP and/or 0.2 mg/Kg VEGF

siRNA. Mice were killed 1 week after the final injection. Lung tissues were fixed in 10% formalin and embedded in paraffin for histological analysis.

In vivo *toxicity.* Twenty-four hours after three daily IV injections, blood was drawn from the venous plexus of the eyes of the mice. Blood samples were immediately centrifuged at 3,000*g* for 5 minutes at 4 °C, and the supernatant blood serums were collected for hematological analysis. Blood urine nitrogen, creatinine, aspartate aminotransferase, and alanine aminotransferase values were recorded, as indications of hepatic and renal functions. Organs (heart, liver, spleen, lung, and kidney) of mice in different treatment groups were fixed and sectioned for H&E staining. Images were collected using a Nikon light microscope (Nikon). For immunotoxicity experiment, mice were given one IV injection of different LCP formulations, and 24 hours later, the cytokines in serum were determined by using enzyme-linked immunosorbent assay kits for IL-6, IL-12, TNF-α, and IFN-γ (BD Biosciences, San Diego, CA).

Statistical analysis. Results were expressed as a mean ± SD. Student's *t*-tests were used to evaluate statistical significance. A result of $P < 0.05$ was considered to be statistically significant.

SUPPLEMENTARY MATERIAL

Figure S1. Histopathology of different organs evaluated by H&E stain.

Figure S2. Tumor uptake of NBD-labeled (GMP+VEGF)-LCP-AA in H460 tumor–bearing mice.

ACKNOWLEDGMENTS

Research was supported by NIH grants CA151652 and CA149363. The authors would like to thank Charlene M Santos, Lei Peng, and Professor Russell J Mumper for their kind help with the establishment of A549 lung orthotopic mouse model. Kelly Racette helped to edit the manuscript. The technology of LCP has been licensed to Qualiber Inc. The authors declared no conflict of interest.

REFERENCES

1. Han, M, Lv, Q, Tang, XJ, Hu, YL, Xu, DH, Li, FZ *et al.* (2012). Overcoming drug resistance of MCF-7/ADR cells by altering intracellular distribution of doxorubicin via MVP knockdown with a novel siRNA polyamidoamine-hyaluronic acid complex. *J Control Release* **163**: 136–144.
2. Saharinen, P, Eklund, L, Pulkki, K, Bono, P and Alitalo, K (2011). VEGF and angiopoietin signaling in tumor angiogenesis and metastasis. *Trends Mol Med* **17**: 347–362.
3. Yancopoulos, GD, Davis, S, Gale, NW, Rudge, JS, Wiegand, SJ and Holash, J (2000). Vascular-specific growth factors and blood vessel formation. *Nature* **407**: 242–248.
4. Zhang, C, Tan, C, Ding, H, Xin, T and Jiang, Y (2012). Selective VEGFR inhibitors for anticancer therapeutics in clinical use and clinical trials. *Curr Pharm Des* **18**: 2921–2935.
5. Poindessous, V, Ouaret, D, El Ouadrani, K, Battistella, A, Mégalophonos, VF, Kamsu-Kom, N *et al.* (2011). EGFR- and VEGF®-targeted small molecules show synergistic activity in colorectal cancer models refractory to combinations of monoclonal antibodies. *Clin Cancer Res* **17**: 6522–6530.
6. Pestourie, C, Tavitian, B and Duconge, F (2005). Aptamers against extracellular targets for *in vivo* applications. *Biochimie* **87**: 921–930.
7. Chames, P, Van Regenmortel, M, Weiss, E and Baty, D (2009). Therapeutic antibodies: successes, limitations and hopes for the future. *Br J Pharmacol* **157**: 220–233.
8. Kamba, T and McDonald, DM (2007). Mechanisms of adverse effects of anti-VEGF therapy for cancer. *Br J Cancer* **96**: 1788–1795.
9. Oguri, T, Achiwa, H, Sato, S, Bessho, Y, Takano, Y, Miyazaki, M *et al.* (2006). The determinants of sensitivity and acquired resistance to gemcitabine differ in non-small cell lung cancer: a role of ABCC5 in gemcitabine sensitivity. *Mol Cancer Ther* **5**: 1800–1806.
10. Waterhouse, DN, Yapp, D, Verreault, M, Anantha, M, Sutherland, B and Bally, MB (2011). Lipid-based nanoformulation of irinotecan: dual mechanism of action allows for combination chemo/angiogenic therapy. *Nanomedicine (Lond)* **6**: 1645–1654.
11. Chauhan, VP, Stylianopoulos, T, Martin, JD, Popovic, Z, Chen, O, Kamoun, WS *et al.* (2012). Normalization of tumour blood vessels improves the delivery of nanomedicines in a size-dependent manner. *Nat Nanotechnol* **7**: 383–388.
12. Chaitanya, GV, Steven, AJ and Babu, PP (2010). PARP-1 cleavage fragments: signatures of cell-death proteases in neurodegeneration. *Cell Commun Signal* **8**: 31.
13. Nuñez, G, Benedict, MA, Hu, Y and Inohara, N (1998). Caspases: the proteases of the apoptotic pathway. *Oncogene* **17**: 3237–3245.
14. Amoh, Y, Li, L, Tsuji, K, Moossa, AR, Katsuoka, K, Hoffman, RM *et al.* (2006). Dual-color imaging of nascent blood vessels vascularizing pancreatic cancer in an orthotopic model demonstrates antiangiogenesis efficacy of gemcitabine. *J Surg Res* **132**: 164–169.
15. Solorzano, CC, Hwang, R, Baker, CH, Bucana, CD, Pisters, PW, Evans, DB *et al.* (2003). Administration of optimal biological dose and schedule of interferon alpha combined with gemcitabine induces apoptosis in tumor-associated endothelial cells and reduces growth of human pancreatic carcinoma implanted orthotopically in nude mice. *Clin Cancer Res* **9**: 1858–1867.
16. Ma, J and Waxman, DJ (2008). Combination of antiangiogenesis with chemotherapy for more effective cancer treatment. *Mol Cancer Ther* **7**: 3670–3684.
17. Liang, Y, Brekken, RA and Hyder, SM (2006). Vascular endothelial growth factor induces proliferation of breast cancer cells and inhibits the anti-proliferative activity of anti-hormones. *Endocr Relat Cancer* **13**: 905–919.
18. Goel, A and Goel, H (2011). Oral leiomyoma extending in retromolar region. *J Indian Soc Pedod Prev Dent* **29**(6 Suppl 2): S61–S65.
19. Zhang, Y, Satterlee, A and Huang, L (2012). *In vivo* gene delivery by nonviral vectors: overcoming hurdles? *Mol Ther* **20**: 1298–1304.
20. Li, J, Chen, YC, Tseng, YC, Mozumdar, S and Huang, L (2010). Biodegradable calcium phosphate nanoparticle with lipid coating for systemic siRNA delivery. *J Control Release* **142**: 416–421.
21. Tseng, YC, Mozumdar, S and Huang, L (2009). Lipid-based systemic delivery of siRNA. *Adv Drug Deliv Rev* **61**: 721–731.
22. Zhang, Y, Kim, WY, Huang, L. (2013). Systemic delivery of gemcitabine triphosphate via LCP nanoparticles for NSCLC and pancreatic cancer therapy. *Biomaterials*.
23. Trédan, O, Galmarini, CM, Patel, K and Tannock, IF (2007). Drug resistance and the solid tumor microenvironment. *J Natl Cancer Inst* **99**: 1441–1454.
24. Hu, CM, Aryal, S and Zhang, L (2010). Nanoparticle-assisted combination therapies for effective cancer treatment. *Ther Deliv* **1**: 323–334.
25. Banerjee, R, Tyagi, P, Li, S and Huang, L (2004). Anisamide-targeted stealth liposomes: a potent carrier for targeting doxorubicin to human prostate cancer cells. *Int J Cancer* **112**: 693–700.
26. Li, J, Yang, Y and Huang, L (2012). Calcium phosphate nanoparticles with an asymmetric lipid bilayer coating for siRNA delivery to the tumor. *J Control Release* **158**: 108–114.
27. Zhang, Y, Wang, X, Wang, J, Zhang, X and Zhang, Q (2011). Octreotide-modified polymeric micelles as potential carriers for targeted docetaxel delivery to somatostatin receptor overexpressing tumor cells. *Pharm Res* **28**: 1167–1178.
28. Kim, HS, Lee, G, John, SW, Maeda, N and Smithies, O (2002). Molecular phenotyping for analyzing subtle genetic effects in mice: application to an angiotensinogen gene titration. *Proc Natl Acad Sci USA* **99**: 4602–4607.